$\mathcal{H}_2$ Control With Time-Domain Constraints: Theory and an Application

Mario Sznaier, Takeshi Amishima, and Tamer Inanc

***Abstract*—In this paper, we study the problem of minimizing the $\mathcal{H}_2$ norm of a given transfer function subject to time-domain constraints on the time response of a different transfer function to a given test signal. The main result of this paper shows that this problem admits a minimizing solution in $\overline{\mathcal{RH}_2}$. Moreover, rational solutions with performance arbitrarily close to optimal can be found by constructing families of approximating problems. Each one of these problems entails solving a finite-dimensional quadratic programming problem whose dimension can be determined before hand. These results are illustrated and experimentally validated by designing a controller for an active vision application.**

***Index Terms*—$\mathcal{H}_2$ control, ℓ^∞ control, active vision, disturbance rejection, optimal control.**

I. Introduction

In many cases, the objective of a control system design can be stated simply as synthesizing an internally stabilizing controller that minimizes the response to some exogenous inputs. When these exogenous inputs are assumed arbitrary but with bounded energy and the outputs are also measured in terms of energy, this problem leads to the minimization of the $\mathcal{H}_\infty$-norm of the closed-loop system. The case where the exogenous inputs are bounded persistent signals and the outputs are measured in terms of the peak time-domain magnitude, leads to the minimization of an $\mathcal{L}^1/\ell^1$-norm. $\mathcal{H}_\infty$-optimal control can now be solved by elegant state-space formulas [21] while $\mathcal{L}^1/\ell^1$-optimal control can be (approximately) solved by finite linear programming [15]–[17], [19]. Finally, the case where the input is a bounded energy signal and performance is measured in terms of the ℓ^∞ norm leads to the generalized $\mathcal{H}_2$ problem [40], also solvable via finite-dimensional convex optimization.

A common practice in engineering is to state some of these performance requirements in terms of the response of the closed-loop system to a given, fixed test input (such as bounds on the rise time, settling time or maximum error to a step). In this case, if the output is measured in terms of its energy the problems leads to the minimization of the closed-loop $\mathcal{H}_2$-norm, extensively studied in the 1960s and 1970s. On the other hand, if the outputs are measured in terms of the peak time-domain magnitude, it leads to the minimization of $\mathcal{L}^\infty/\ell^\infty$-norm [5], [18], [22], [34], [48], [61].

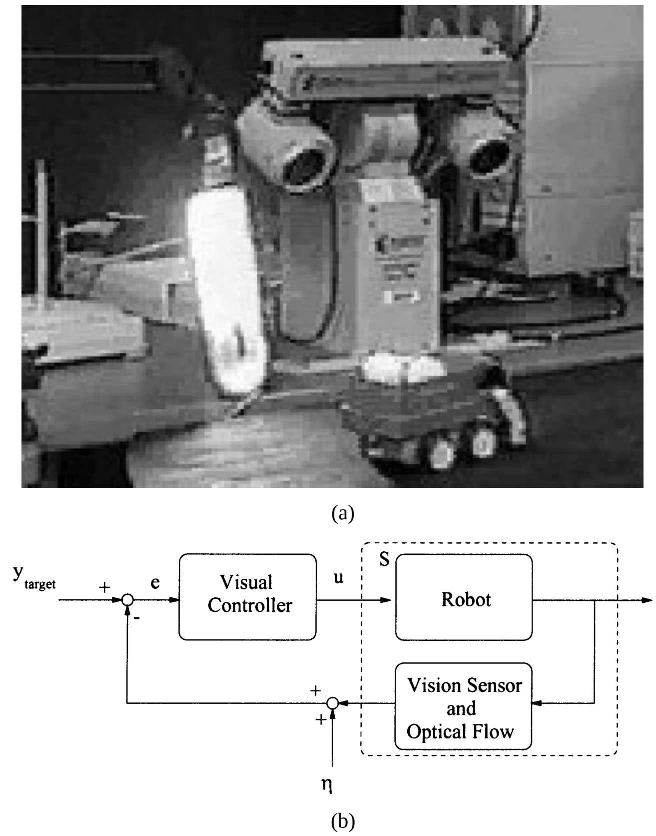

Fig. 1. (a) Visual tracking setup. (b) Corresponding block diagram.

In general, a realistic control problem is likely to involve specifications on both the energy and peak values of the output. Consider for example the problem of smooth tracking of a noncooperative target, illustrated in Fig. 1. Here, the goal is to internally stabilize the plant and to track target motions, $y_{\rm target}$, using as measurements images possibly corrupted by noise η. As indicated in [28], [39], in principle this problem can be solved using LQG control theory.

Fig. 2 shows the experimental response to a step displacement of the target of 25 pixels achieved by an optimal $\mathcal{H}_2$ controller. This controller was designed using a stable, nonminimum-phase model of the combined dynamics of the head and vision sensor, obtained via control oriented identification (see Section V for details). Note that the tracking error settles to ± 4 pixels (within the experimental measurement error) in approximately one second. However, the control action has large oscillations, leading to jerky motions that create significant stress on the pan and tilt unit. Moreover, the error response also exhibits

Manuscript received May 2, 2000; revised April 13, 2001, March 18, 2002, and July 9, 2002. Recommended by Associate Editor B. M. Chen. This work was supported in part by the National Science Foundation under Grants ECS-9907051 and IIS-0117387, and by the Air Force Office of Scientific Research under Grant F49620-00-1-0020.

The authors are with the Department of Electrical Engineering, The Pennsylvania State University, University Park, PA 16802 USA (e-mail: msznaier@gandalf.ee.psu.edu; takeshi@gandalf.ee.psu.edu; tinanc@gandalf.ee.psu.edu).

Digital Object Identifier 10.1109/TAC.2003.809143

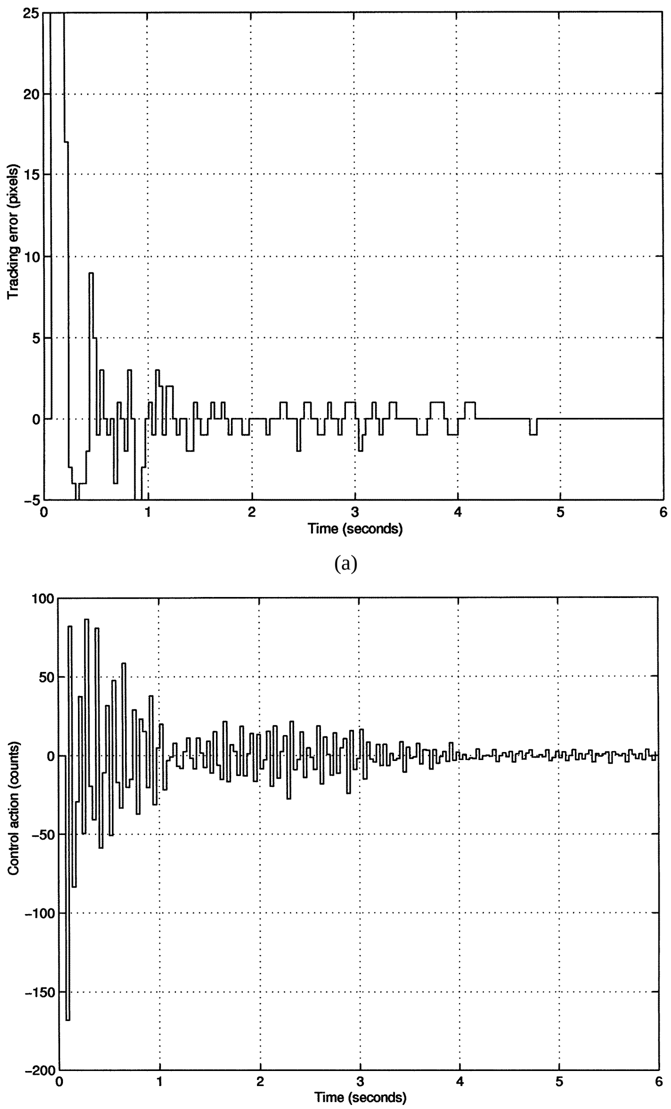

(a)

(b)

Fig. 2. (a) Tracking error to a step input (experimental). (b) Control action.

significant undershoot and oscillations. Our goal is to design a controller that substantially decreases the peak value of the control action and the oscillations in the error response, while achieving comparable tracking performance in terms of the root mean square (RMS) value of the error.

It is well known that, for discrete-time stable systems, the $\mathcal{H}_2$ norm is an upper bound of the ℓ^∞ norm. Thus, in principle one can try to enforce restrictions on the peak value of a (weighted) time-domain response through the minimization of a weighted $\mathcal{H}_2$ norm. However, this approach can be arbitrarily conservative. State and control constraints can be handled by rendering appropriate sets positively invariant (see for instance [10], [20], [52], [59] and the excellent survey [7]). LQR control subject to input constraints has been addressed in [25], [62] using ellipsoidal invariant sets. However, these methods are potentially conservative, due to the choice of invariant sets and are restricted to the state feedback case. Alternatively, these problems can be addressed using receding horizon-type methods [11], [36], [42], [50], [51]. However, stability considerations require the on-line solution of a constrained optimization problem, which limits the applicability of the method in situations like the previous one, with relatively fast sampling times (33 ms).

$\mathcal{H}_2$ control problems with time-domain constraints can be addressed by recasting them into a mixed $\mathcal{H}_2/\ell^1$ optimization form and elegantly solved using the methods proposed in [41]. However, this is a worst-case type approach that guarantees satisfaction of the time-domain constraints for all signals in the ℓ^∞–unit ball. Thus, these controllers are potentially very conservative for applications such as the active vision problem discussed above, where the specifications are given in terms of the response to a few test signals, representing the typical patterns of motion of the target.

In this paper, motivated by the results in [47], we propose a solution to both, continuous and discrete time $\mathcal{H}_2$ problems subject to time domain constraints given in terms of the response to a set of fixed, given signals. Specifically, the contributions of this paper are as follows.

- Establishing that contrary to some other multiobjective problems such as mixed $\mathcal{H}_2/\mathcal{H}_\infty$, $\mathcal{H}_2$ problems with time domain constraints admit a solution in $\overline{\mathcal{RH}_2}$, the closure of the subspace of $\mathcal{H}_2$ formed by real rational transfer matrices.
- A computational procedure, based on finite-dimensional quadratic programming, to compute ϵ-suboptimal real rational (and, thus, implementable) controllers.
- Extension of these results to the continuous time case.
- Experimental validation of the theory with a nontrivial application.

The paper is organized as follows. In Section II, we introduce the notation to be used and some preliminary results. In Section III, we introduce two modified $\mathcal{H}_2/\ell^\infty$ problems, providing suboptimal and a super-optimal solutions respectively. Both problems can be reduced to finite dimensional quadratic programming, and in the limit their respective solutions strongly converge to the solution of the original problem. In Section IV, we solve the continuous-time counterpart of the problem. The theory is illustrated in Section V by synthesizing and experimentally validating a controller for the active vision application mentioned above. Finally, in Section VI, we summarize our results and we indicate directions for future research.

II. Preliminaries

In this section, we introduce the notation used in the paper, precisely state the problem under consideration, and present preliminary results that will be latter used to reduce this problem to a finite-dimensional convex optimization.

A. Notation

The notation used in this paper is summarized here.

$R(R_+)$ Set of real (positive real) numbers.

$\ell_1^{m\times n}$ Banach space of matrix valued right-sided, absolutely summable real sequences $x = \{x(k)\}_{k=0}^\infty$ equipped with the norm $\|x\|_{\ell_1} \doteq \max_{1\leq i\leq m} \sum_{j=1}^n \sum_{k=0}^\infty |x_{ij}(k)| < \infty$.

$\ell_1(Z)$ Banach space of absolutely summable, double sided real sequences $\{x_n\}$ equipped with the norm $\|x\|_{\ell_1} = \sum_{n=-\infty}^{n=\infty} |x_n|$.

$\ell_2^{m\times n}$ Hilbert space of matrix valued right-sided, energy bounded real sequences $x = \{x(k)\}_{k=0}^{\infty}$ equipped with the norm $\|x\|_{\ell_2} \doteq \left(\sum_{i=1}^{m}\sum_{j=1}^{n}\sum_{k=0}^{\infty}|x_{ij}(k)|^2\right)^{1/2} < \infty$.

$\ell_\infty^{m\times n}$ Banach space of matrix valued right-sided, bounded sequences $x = \{x(k)\}_{k=0}^{\infty}$ equipped with the norm $\|x\|_{\ell_\infty} = \max_{1\le j\le n}\sum_{i=1}^{m}\sup_{k\ge 0}|x_{ij}(k)| < \infty$.

ℓ_g^m Space of real vector sequences $\{x(k)\} \in \ell_\infty^m$ such that $\{x_i(k)/g_i(k)\} \in \ell_\infty$, equipped with the norm $\|x\|_{g,\infty} = \max_{1\le i\le m}\sup_{k\ge 0}|g_i^{-1}(k)x_i(k)|$, where $g(k) \in \ell_\infty^m$ is a given sequence, such that $g_i(k) > 0$.

$\mathcal{L}_2^{m\times n}(R_+)$ Hilbert space of matrix valued Lebesgue integrable functions $x(t)$ on R_+ equipped with the norm $\|x\|_{\mathcal{L}_2} \doteq \left(\sum_{i=1}^{m}\sum_{j=1}^{n}\int_0^\infty |x_{ij}(t)|^2 dt\right)^{1/2} < \infty$.

$\mathcal{L}_\infty^{m\times n}(R_+)$ Banach space of matrix valued Lebesgue integrable functions $x(t)$ on R_+ with the norm $\|x\|_{\mathcal{L}_\infty} \doteq \max_{1\le j\le n}\sum_{i=1}^{m}\operatorname{esssup}_{t\in R_+}|x_{ij}(t)| < \infty$.

$\mathcal{H}_2^{m\times n}(j\omega)$ Hilbert space of matrix valued complex functions $F(s)$ with analytic continuation on the open right—half plane, and square integrable there, equipped with the usual $\mathcal{H}_2$ norm $\|F\|_{\mathcal{H}_2}^2 \doteq 1/2\pi\int_{-\infty}^{\infty} Trace\,[F^*(j\omega)F(j\omega)]\,d\omega < \infty$.

$\mathcal{H}_2^{m\times n}(D)$ Discrete time counterpart of $\mathcal{H}_2(j\omega)$, i.e., Hilbert space of matrix valued complex functions $F(\lambda)$ with analytic continuation inside the unit disk, equipped with the norm $\|F\|_{\mathcal{H}_2}^2 \doteq 1/2\pi\int_{-\pi}^{\pi} Trace\left[F^*(e^{j\theta})F(e^{j\theta})\right] d\theta$.

λ λ transform of a right—sided real sequence: $X(\lambda) = \sum_{i=0}^{\infty} x_i\lambda^i$.

$\mathcal{P}_n$ $\mathcal{P}_n\left[\sum_{i=0}^{\infty} G_i\lambda^i\right] \doteq \sum_{i=0}^{n-1} G_i\lambda^i$.

$\tilde{G}$ Conjugate of an operator: $\tilde{G} = G^T(1/\lambda)$.

$\|\cdot\|_F$ Frobenious norm: for $M \in R^{m\times n}$, $\|M\|_F^2 = \sum_{i,j} m_{i,j}^2$.

B. $\mathcal{H}_2$ With Time Domain Constraints Problem

Consider the system shown in Fig. 3, where the signals $w_t \in R^{n_{w_t}}$ and $w_2 \in R^{n_{w_2}}$ represent known test signals and exogenous disturbances, respectively, and where $z_t \in R^{n_{z_t}}$ and $z_2 \in R^{n_{w_2}}$ represent regulated outputs. Our goal is to find an internally stabilizing control law $u = Ky$, $u \in R^{n_u}$, $y \in R^{n_y}$ that minimizes the $\mathcal{H}_2$ norm of the closed-loop transfer function from w_2 to z_2, subject to time domain constraints on the response of some of the elements of z_t to test signals $w_t \in \mathcal{W}_t$, of the form

$$|z_{t_i}(k)| \le \phi_i(k)$$

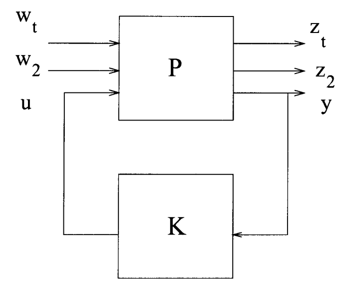

Fig. 3. $\mathcal{H}_2$ with time domain constraints setup.

where $\{\phi_i(k)\}$ is a given ℓ^∞ sequence. A typical choice for $\phi_i(\cdot)$ is

$$\begin{aligned}\phi(k) &= M, \qquad k = 0, 1, \ldots, k_1\\ \phi(k) &= Ma^{(k-k_1)}, \qquad k_1 \le k,\ \ 0 < a < 1.\end{aligned} \tag{2-1}$$

This sequence imposes constraints on the maximum overshoot (M) and forces exponential decay of the output after time k_1.

In the sequel, we will assume without loss of generality (by using superposition if necessary) that the test signals in the set $\mathcal{W}_t$ are of the form $w_t^j(k) = [0 \quad 0 \quad \ldots \quad w_j(k) \quad \ldots \quad 0]^T$. Moreover, by using weighting functions and absorbing these weights in the generalized plant (see [61] for details) it can also be assumed that $w_j(k)$ is an impulse.

Let $T(\lambda)$ and $S(\lambda)$ denote the closed-loop transfer matrices from w_2 to z_2 and from w_t to z_t respectively, obtained when connecting a stabilizing controller from y to u. Using the Youla Parameterization, the set of all such transfer matrices can be parameterized by [63]

$$\begin{aligned}T &= T^{11} + T^{12}QT^{21}\\ S &= S^{11} + S^{12}QS^{21}\end{aligned} \tag{2-2}$$

where $Q \in \mathcal{H}_2^{n_u\times n_y}$, $T^{11} \in \ell_1^{n_{z_2}\times n_{w_2}}$, $T^{12} \in \ell_1^{n_{z_2}\times n_u}$, $T^{21} \in \ell_1^{n_y\times n_{w_2}}$, $S^{11} \in \ell_1^{n_{z_t}\times n_{w_t}}$, $S^{12} \in \ell_1^{n_{z_t}\times n_u}$, and $S^{21} \in \ell_1^{n_y\times n_{w_t}}$. Moreover, by suitable selecting the parametrization, without loss of generality it can be assumed that the transfer matrices T^{ij} and S^{ij} are analytic inside the disk $|\lambda| \le (1/a) < \rho$. In order to stress the dependence on Q, the notations $T(Q)$ and $S(Q)$ are sometimes used in the sequel.

The parameterization allows for precisely stating the $\mathcal{H}_2$ with time-domain constraints problem as follows.

Problem 1: Given sequences $\{\phi_{i,j}(k)\}$ of the form (2-1), find the optimal value of the performance measure

$$\mu \doteq \inf_{Q\in\mathcal{H}_2^{n_u\times n_y}} \|T^{11} + T^{12}QT^{21}\|_{\mathcal{H}_2}^2 \tag{2-3}$$

subject to

$$\begin{aligned}\|S(Q)_{i,j}\|_{\phi_{i,j},\infty} \doteq \left\|\frac{S(Q,k)_{i,j}}{\phi_{i,j}(k)}\right\|_{\ell^\infty} &\le 1\\ k = 0, 1, 2, \ldots, \{i,j\} &\in \mathcal{I}\end{aligned} \tag{2-4}$$

and the corresponding controller Q_{opt}, where $\mathcal{I}$ denotes the set of input–output pairs subject to time domain constraints.

Next, we show that under mild conditions, the solution to this problem is unique.

Lemma 1: Let T^{12}, T^{21} have generically full column and row rank respectively, and assume that a solution to problem 1 exists. Then, this solution is unique.

Proof: Let Q_1 and Q_2 solve Problem 1, and assume by contradiction that $Q_1 \neq Q_2$. By the strict convexity of the $\mathcal{H}_2$ norm $T^{11}+T^{12}Q_1T^{21} = T^{11}+T^{12}Q_2T^{21}$. Since by assumption T^{12} has full-column rank and T^{21} has full-row rank, necessarily $Q_1 = Q_2$.

In the sequel, we solve Problem 1 by constructing sequences of super and suboptimal controllers, $\{\underline{Q^i}\}$ and $\{\overline{Q^i}\}$, such that $\|T(\underline{Q^i})\|_2 \uparrow \mu$ and $\left\|T(\overline{Q^i})\right\|_2 \downarrow \mu$, respectively. Moreover, these controllers can be found by solving finite-dimensional quadratic programming problems. in order to establish these facts, we need the following result, showing that the components of every feasible controller Q that are relevant to the time-domain constraints are bounded in the ℓ^∞ sense.

Given an input–output pair $(i,j) \in \mathcal{I}$ subject to time-domain constraints, denote by S_i^{12} and S_j^{21} the $i^{\rm th}$ row and $j^{\rm th}$ column of S^{12} and S^{21}, respectively. By considering the corresponding Smith–Mcmillan decompositions [33], it follows that there exist unimodular (i.e., polynomial with polynomial inverse) matrices V_j^L and V_i^R such that

$$\begin{aligned} S_i^{12} =& [0 \quad 0 \quad \dots \quad \tilde{S}_i^{12}(\lambda) \quad \dots \quad 0]\, V_i^R(\lambda);\\ S_j^{21} =& V_J^L(\lambda) \begin{bmatrix} 0\\ 0\\ \vdots\\ \tilde{S}_j^{21}(\lambda)\\ \vdots\\ 0 \end{bmatrix}. \end{aligned} \tag{2-5}$$

Hence, the constraint (2-4) is equivalent to

$$\left\| S_{ij}^{11} + \tilde{S}_i^{12}\tilde{S}_j^{21}\tilde{Q}_{ij} \right\|_{\phi_{ij},\infty} \leq 1 \tag{2-6}$$

where $\tilde{Q}_{ij} = \left(V_i^R Q V_j^L\right)_{i,j}$.

Lemma 2: Assume that $S_i^{12}(\lambda)$, $S_j^{21}(\lambda)$ have full row and column rank on $|\lambda| = 1$. Then, all feasible controllers satisfy $\|\tilde{Q}_{ij}\|\ell^\infty \leq M_{ij}$, where M_{ij} depends only on the problem data.

Proof: Since S_i^{12} and S_j^{21} have full row and column rank on $|\lambda| = 1$ it follows that $(\tilde{S}_i^{12}\tilde{S}_j^{21})(\lambda) \neq 0$ on the unit circle. Thus, Wiener–Gelfand's theorem [13] implies that $S^\dagger = (\tilde{S}_i^{12}\tilde{S}_j^{21})^{-1} \in \ell^1(Z)$. It follows that if Q is feasible for Problem 1, then:

$$\begin{aligned} \|\tilde{Q}_{ij}\|\ell^\infty =& \|S^\dagger \tilde{S}_i^{12}\tilde{S}_j^{21}\tilde{Q}_{ij}\|\ell^\infty \leq \|S^\dagger\|_{\ell^1}\|\tilde{S}_i^{12}\tilde{S}_j^{21}\tilde{Q}_{ij}\|\ell^\infty\\ \leq& \|S^\dagger\|_{\ell^1}\left(\|\phi\|\ell^\infty + \|S_{ij}^{11}\|\ell^\infty\right) \doteq M_{ij}. \end{aligned} \tag{2-7}$$

III. Problem Solution

In this section, we show that Problem 1 can be solved by solving two modified $\mathcal{H}_2/\ell^\infty$ problems, providing suboptimal and a superoptimal solutions respectively. Both problems can be reduced to finite dimensional quadratic programming, and in the limit their respective solutions strongly converge, in the $\mathcal{H}_2$ topology, to the solution of the original problem.

A. Problem Transformation

It is a standard result (see, for instance [53, p. 194]) that the parameterization of all stabilizing controllers can be selected (by redefining Q if necessary), so that T^{12} and T^{21} are inner and co-inner, respectively. Thus, there exist $T^{12\perp}$, $T^{21\perp}$ such that $[\,T^{12} \quad T^{12\perp}\,]$ and $\begin{bmatrix} T^{21}\\ T^{21\perp}\end{bmatrix}$ are unitary. Let

$$\begin{aligned} R^{11} \doteq& T^{12\sim}T^{11}T^{21\sim}\\ R^{12} \doteq& T^{12\sim}T^{11}T^{21\perp\sim}\\ R^{21} \doteq& T^{12\perp\sim}T^{11}T^{21\sim}\\ R^{22} \doteq& T^{12\perp\sim}T^{11}T^{21\perp\sim}. \end{aligned} \tag{3-1}$$

Through straightforward but tedious operations, it can be shown ([53, p. 195]) that with this choice of the parametrization, $R^{ij} \in \mathcal{RH}_2^\perp$. Since the $\mathcal{H}_2$ norm is invariant under pre- (post) multiplication by unitary matrices, we have that

$$\begin{aligned} \left\|T^{11}+T^{12}QT^{21}\right\|_{\mathcal{H}_2}^2 =& \left\|\begin{bmatrix} R^{11}+Q & R^{12}\\ R^{21} & R^{22}\end{bmatrix}\right\|_{\mathcal{H}_2}^2\\ =& \left\|\begin{bmatrix} R^{11sp} & R^{12}\\ R^{21} & R^{22}\end{bmatrix}\right\|_{\mathcal{H}_2}^2\\ &+ \left\|\begin{bmatrix} D^{R^{11}}+Q & 0\\ 0 & 0\end{bmatrix}\right\|_{\mathcal{H}_2}^2\\ =& \left\|\begin{bmatrix} R^{11sp} & R^{12}\\ R^{21} & R^{22}\end{bmatrix}\right\|_{\mathcal{H}_2}^2\\ &+ \left\|D^{R^{11}}+Q\right\|_{\mathcal{H}_2}^2 \end{aligned} \tag{3-2}$$

where R^{11sp} and $D^{R^{11}}$ denote the strictly proper part of R^{11} and its feed through term, respectively. Thus, Problem 1 may be reformulated as follows.

Problem 2: Find the optimal value of the performance measure

$$\inf_{Q^n \in \mathcal{H}_2^{n_u \times n_y}} \|Q^n\|_{\mathcal{H}_2}^2 \text{ subject to}$$
$$\left\|\left[S^{11}+S^{12}(Q^n - D^{R^{11}})S^{21}\right]_{rs}\right\|_{\phi_{rs},\infty} \leq 1. \tag{3-3}$$

Problem 2 is a convex infinite-dimensional problem, for which no closed-form solution is known to exist. In this paper, a solution will be computed by taking the limit of the solution to some finite-dimensional minimization problems. In the sequel, we will assume without loss of generality (by redefining S^{11} as $S^{11} - S^{12}D^{R^{11}}S^{21}$, if necessary) that $D^{R^{11}} = 0$.

B. Computation of Superoptimal Solutions

In this section, a sequence of finite-dimensional convex optimization problems is introduced. The nth problem has $\mathcal{O}(n)$ variables, and its optimal cost μ^n satisfies $\mu^n \leq \mu$. The sequence of problems approximates Problem 1 in the sense that $\mu^n \to \mu$ and the partial solutions converge to the optimal solution (in the $\mathcal{H}_2$ norm) as $n \to \infty$.

Using the projection operator $\mathcal{P}_n$, consider the optimization problem

Problem 3: Find the optimal value of the performance measure

$$\underline{\mu}^n = \inf_{Q^n \in \mathcal{H}_2{}^{n_u \times n_y}} \|Q^n\|^2_{\mathcal{H}_2} \text{ subject to } \left\|\mathcal{P}_n(S^{11} + S^{12}Q^nS^{21})_{rs}\right\|_{\phi_{rs},\infty} \leq 1. \tag{3-4}$$

Problem 3 can be thought of as a finitely-many constraints approximation to the original problem, where the constraints are enforced only over a finite horizon n. In the sequel, we show that this problem is equivalent to a finite dimensional quadratic programming problem.

Lemma 3: Problem 3 is equivalent to

$$\underline{\mu}^n = \min_{[Q^n(0) \quad Q^n(1) \quad \cdots \quad Q^n(n-1)]} \sum_{i=0}^{n-1} \|Q^n(i)\|^2_F \text{ subject to:} \tag{3-5}$$

$$\left\|\mathcal{P}_n\left[S^{11}(\lambda) + S^{12}(\lambda)\left(\sum_{i=0}^{n-1} Q^n(i)\lambda^i\right)S^{21}\right]_{rs}\right\|_{\phi_{rs},\infty} \leq 1. \tag{3-6}$$

Proof: Follows from the fact that for any feasible $Q \in \mathcal{H}_2{}^{n_u \times n_y}$ we have that $Q^n = \mathcal{P}_n(Q)$ is also feasible and yields a lower cost.

Theorem 1: Assume that there exists $\hat{Q} \in \mathcal{H}_2{}^{n_u \times n_y}$ such that $\|(S^{11} + S^{12}\hat{Q}S^{21})_{rs}\|_{\phi_{rs},\infty} \leq 1$. Then, $\underline{\mu}^n \uparrow \mu$ and $\|Q^n - Q_{\text{opt}}\|_{\mathcal{H}_2} \to 0$, where $Q_{\text{opt}} \in \mathcal{H}_2{}^{n_u \times n_y}$ is the solution to Problem 1.

Proof: To show that $\underline{\mu}^n \uparrow \mu$ note that if Q^{n+1} solves Problem 3 with horizon $n+1$ then it is feasible for Problem 3 with horizon n. Thus $\underline{\mu}^n \leq \underline{\mu}^{n+1}$. Since $\underline{\mu}$ is bounded above by $\|\hat{Q}\|_{\mathcal{H}_2}$, it follows that the sequence $\{\underline{\mu}^n\}$ has a limit $\underline{\mu}_{\text{lim}} \leq \mu$. To establish that $\underline{\mu}_{\text{lim}} = \mu$ we will find a feasible $Q \in \mathcal{H}_2{}^{n_u \times n_y}$ such that $\|Q\|_{\mathcal{H}_2} = \mu_{\text{lim}}$.

Given any n, m, $m > n$, define $Q^{nm} = 0.5 * (Q^n + Q^m)$. From convexity, we have that Q^{nm} is feasible for Problem 3 with horizon n. Moreover

$$\begin{aligned}\|Q^n - Q^m\|^2_{\mathcal{H}_2} =& 2\|Q^n\|^2_{\mathcal{H}_2} + 2\|Q^m\|^2_{\mathcal{H}_2} - 4\|Q^{mn}\|^2_{\mathcal{H}_2} \\ \leq& 4\left[(\underline{\mu}^m)^2 - (\underline{\mu}^n)^2\right].\end{aligned} \tag{3-7}$$

Thus, as $n, m \to \infty$, $\|Q^n - Q^m\|_{\mathcal{H}_2} \to 0$. This establishes the fact that Q^n is a Cauchy sequence and, therefore, (since $\mathcal{H}_2$ is complete) it converges strongly to some $Q^* \in \mathcal{H}_2{}^{n_u \times n_y}$, with $\|Q^*\|_{\mathcal{H}_2} = \mu_{\text{lim}}$. Next, we show that Q^* is feasible for Problem 1. To this effect, note that strong convergence of Q in the $\mathcal{H}_2$ topology, implies that $\|S(Q^n)_{rs} - S(Q^*)_{rs}\|_{\mathcal{H}_2} \to 0$, which in turn implies strong convergence of $S(Q^n)_{rs}$ to $S(Q^*)_{rs}$ in the ℓ^∞ topology. Thus, if Q^* is not feasible, there exist some finite κ and N such that

$$\left|\left(S^{11} + S^{12}Q^nS^{21}\right)_{rs}(\kappa)\right| > \phi_{rs}(\kappa) \text{ for all } n > N. \tag{3-8}$$

However, this contradicts (3-6) for $n \geq \max\{N, \kappa\}$.

C. Computation of Suboptimal Solutions

Theorem 1 shows that a solution to Problem 1 can be obtained by solving a sequence of quadratic programming problems. However, it does not furnish information on how to select n to achieve some desired error bound. To solve this difficulty, in this section we introduce a sequence of suboptimal solutions converging to the optimal from above. Solutions to Problem 1 with arbitrary accuracy can then be found by computing upper and lower bounds of μ until the difference between these bounds is as small as desired.

Consider the following finitely many variables approximation to Problem 1.

Problem 4:

$$\overline{\mu}^n = \min_{[Q^n(0) \quad Q^n(1) \quad \cdots \quad Q^n(n-1)]} \sum_{i=0}^{n-1} \|Q^n(i)\|^2_F$$
$$\text{s.t. } \left\|\left[S^{11}(\lambda) + S^{21}(\lambda)Q^n(\lambda)S^{21}(\lambda)\right]_{rs}\right\|_{\phi_{rs},\infty} \leq 1$$

where $Q^n(\lambda) = \sum_{i=0}^{n-1} Q^n(i)\lambda^i$.

Theorem 2: Assume that there exists $\hat{Q} \in \mathcal{H}_2{}^{n_u \times n_y}$ such that $\|S(\hat{Q})\|_{\phi,\infty} \leq 1$. Then $\overline{\mu}^n \downarrow \mu$ and $\|Q^n - Q_{\text{opt}}\|_{\mathcal{H}_2} \to 0$, where $Q_{\text{opt}} \in \mathcal{H}_2{}^{n_u \times n_y}$ is the solution to Problem 1.

Proof: If Q^n solves Problem 4 with horizon n then it is also feasible with horizon $n+1$. Thus $\overline{\mu}_n \geq \overline{\mu}_{n+1}$. Since the sequence $\{\overline{\mu}_n\}$ is bounded below by μ, it follows that it has a limit $\overline{\mu}_{\text{lim}} \geq \mu$. Proceeding as in the proof of Theorem 1 it can be shown that $\{Q^n\}$ is a Cauchy sequence and, thus, it converges to some $\bar{Q}^* \in \mathcal{H}_2$. As before, it can be easily shown that $\bar{Q}^*$ is feasible. Finally, from Lemma 1 we have that $\bar{Q}^* = Q_{\text{opt}}$.

In principle, Problem 4 is a semi-infinite-dimensional quadratic programming problem, since it has an infinite number of constraints. However, as we show in the sequel, under mild conditions only finitely many of these constraints are active.

Theorem 3: Let $\mathcal{I}$ denote the set of pairs (r, s) such that $S(Q)_{rs}$ is subject to time-domain constraints. Denote by S^{12}_r and S^{21}_s the r^{th} row and s^{th} columns of S^{12} and S^{21}, and assume that S^{12}_r and S^{21}_s have full row and column rank on $\lambda = 1$, respectively, for all pairs $(r, s) \in \mathcal{I}$. Then, Problem 4 is equivalent to

$$\overline{\mu}^n = \min_{[Q^n(0) \quad Q^n(1) \quad \cdots \quad Q^n(n-1)]} \sum_{i=0}^{n-1} \|Q^n(i)\|^2_F$$
$$\text{subject to}$$
$$\left\|\mathcal{P}_{N_1}\left[S^{11}(\lambda) + S^{12}(\lambda)Q^n(\lambda)S^{21}(\lambda)\right]_{rs}\right\|_{\phi_{rs},\infty} \leq 1 \tag{3-9}$$

$$\left|\left(V^R_iQ^nV^L_j\right)_{i,j}(k)\right| \leq M_Q, \quad k = 0, 1 \ldots, N_2 - 1 \quad (i, j) \in \mathcal{I} \tag{3-10}$$

where $Q^n(\lambda) = \sum_{i=0}^{n-1} Q^n(i)\lambda^i$, M_Q, $N_1(n)$ and $N_2(n)$ are constants that depend only on the problem data and the length of the finite-impulse response (FIR) Q, and the unimodular matrices V^R_i, V^L_j are defined in (2-5).

Proof: For notational simplicity, let $\tilde{Q}_{ij} = (V^R_iQ^nV^L_j)_{i,j}$ and $\tilde{S}_{ij} = \tilde{S}^{12}_i\tilde{S}^{21}_j$. Since V^R_i, V^L_j and Q^n are polynomial matrices, it follows that there exist some $N_2(n)$ such that $\tilde{Q}_{ij}(k) = 0$, for all $k \geq N_2$ and $(i, j) \in \mathcal{I}$. From Lemma 2 we have that every feasible controller satisfies a bound of the form

$$|\tilde{Q}_{i,j}(k)| \leq M_{i,j}.$$

Thus defining $M_Q = \max\{M_{i,j}\}$ renders the additional constraint (3-10) redundant at the optimum. Moreover, since the

Youla parametrization is chosen so that $S^{i,j}$ is analytic in $|\lambda| \leq (1/a) < \rho$, there exists $N_3(n, N_2)$ (that can be precomputed *a priori*) such that $|S_{rs}^{11}(k)| + \|(I - \mathcal{P}_{(k-N_2+1)})\tilde{S}_{rs}\|_{\ell^1} * M_Q \leq \phi_{rs}(k)$ for all $k \geq N_3$. The proof follows now by noting that, for all $k \geq N_1 = \max\{N_2, N_3\}$, we have

$$\begin{aligned}\left|(S^{11} + S^{12}QS^{21})_{rs}(k)\right| =& \left|(S_{rs}^{11} + \tilde{S}_{rs}\tilde{Q}_{rs})(k)\right| \\ \leq& |S_{rs}^{11}(k)| \\ &+ \sum_{l=0}^{N_2-1} \left|\tilde{S}_{rs}(k-l)\|\tilde{Q}ij(l)\right| \\ \leq& |S_{rs}^{11}(k)| \\ &+ \left\|(I - \mathcal{P}_{(k-N_2+1)})\tilde{S}_{rs})\right\|_{\ell^1} \\ &\times M_{rs} \\ \leq& \phi_{rs}(k) \end{aligned} \tag{3-11}$$

i.e., all the constraints are automatically satisfied for $k \geq N_1$.

IV. Continuous-Time Case

In this section, we consider the continuous-time counterpart of Problem 1, as follows.

Problem 5: Given functions $\phi_{rs}(t) > 0$ of the form

$$\phi_{rs}(t) = \begin{cases} M & 0 \leq t \leq t_o \\ Me^{-(t-t_o)/\tau_o} & t > t_o \end{cases} \tag{4-1}$$

find the optimal value of the performance measure

$$\begin{aligned}\mu_t \doteq& \inf_{Q \in \mathcal{H}_2} \|Q\|_2 \text{ subject to } |(S_{rs}(t)| \leq \phi_{rs}(t) \\ t \geq& 0, \quad (r, s) \in \mathcal{I}\end{aligned} \tag{4-2}$$

and the corresponding optimal controller Q^*.

The main result of this section shows that this problem can be solved by solving a sequence of discrete-time problems similar to Problem 1. In the sequel, we consider, for notational simplicity, single-input–single-output (SISO) systems but the technique extends trivially to the multiple-input–multiple-output case.

Given a continuous-time system with state-space realization

$$G(s) = \left(\begin{array}{c|c} A & B \\ \hline C & 0 \end{array}\right) \tag{4-3}$$

we define its Euler approximating system (EAS) as the following *discrete-time* system:

$$G_E(z) = \left(\begin{array}{c|c} I + \tau A & \tau B \\ \hline C & 0 \end{array}\right). \tag{4-4}$$

The EAS approach has been used in the past [6], [48] to solve continuous-time $\mathcal{L}^1$ and mixed $\mathcal{L}_\infty/\mathcal{H}_\infty$ problems by reducing them to solving equivalent discrete-time control problems. From the properties of the EAS (see Lemmas 5 and 4 in the Appendix), it can be easily seen that, if $\Phi_{rs}(t)$ is constant then a solution to Problem 5 with cost arbitrarily close to the optimal can be found by considering a sequence $\tau_i \downarrow 0$ and solving a sequence discrete-time problems of the form

$$\mu_i = \min \|Q_E(\tau_i)\|_2 \text{ subject to } \|S_E(Q_E, \tau_i)\|_{\ell^\infty} \leq \tau_i \phi \tag{4-5}$$

where Q_E and S_E denote the EAS of Q and $S^{11} + S^{12}QS^{21}$, respectively. As we show next, the same approach can be used for constraints of the form (4-1).

Lemma 4: Consider the strictly proper stable system (4-3) and its corresponding EAS (4-4). Denote by $g(t)$ and $g_E(k, \tau)$ the respective impulse responses. Then, the following hold.

1) Given $0 < \tau < \tau_o$, if $|g_E(k, \tau)| \leq \phi\,(1 - (\tau/\tau_o))^{k-1}$, then $|g(t)| \leq \phi e^{-(t/\tau_o)}$.
2) If for all $0 < \tau < \tau_o$ there exist $k(\tau)$ and ϵ such that $|g_E[k(\tau), \tau]| > \phi\,(1 - (\tau/\tau_o))^{k(\tau)-1} + \epsilon$, then there exist $\tilde{t}$ such that $|g(\tilde{t})| > \phi e^{-(\tilde{t}/\tau_o)}$.

Proof: Let $\tilde{g} = g(t)e^{t/\tau_o}$. Given $\tau < \tau_o$ define τ_{eq} by

$$\frac{1}{\tau_{eq}} = \frac{1}{\tau} - \frac{1}{\tau_o}. \tag{4-6}$$

It can be easily seen that the EAS system of $\tilde{g}$ corresponding to τ_{eq} has the following state-space realization:

$$\begin{aligned}\tilde{G}_E(z, \tau_{eq}) &= \left(\begin{array}{c|c} I + \tau_{eq}\left(A + \frac{I}{\tau_o}\right) & \tau_{eq}B \\ \hline C & 0 \end{array}\right) \\ &= \left(\begin{array}{c|c} \left(1 + \frac{\tau_{eq}}{\tau_o}\right)(I + \tau A) & \tau_{eq}B \\ \hline C & 0 \end{array}\right).\end{aligned} \tag{4-7}$$

From Property 5 in Lemma 5 in the Appendix, it follows that

$$|\tilde{g}_E(k, \tau_{eq})| \leq \tau_{eq}\phi \quad \forall k \Rightarrow |\tilde{g}(t)| \leq \phi \iff |g(t)| \leq \phi e^{-(t/\tau_o)}. \tag{4-8}$$

The proof of Property 1 follows now from the relationship between the Markov parameters of $\tilde{G}_E(\tau_{eq})$ and $G_E(\tau)$

$$\begin{aligned}\tilde{g}_E(k, \tau_{eq}) =& \tau_{eq}C\left(1 + \frac{\tau_{eq}}{\tau_o}\right)^{k-1}(I + \tau A)^{k-1}B \\ =& \tau_{eq}C\left(1 - \frac{\tau}{\tau_o}\right)^{-(k-1)}(I + \tau A)^{k-1}B \\ =& \tau_{eq}\left(1 - \frac{\tau}{\tau_o}\right)^{-(k-1)}g_E(k, \tau).\end{aligned} \tag{4-9}$$

Property 2 now follows from the aforementioned derivation, combined with Property 5 in Lemma 5 and the fact that $\tau_{eq} \downarrow 0$ as $\tau \downarrow 0$.

Corollary 1: A solution to Problem 5 with cost arbitrarily close to the optimal can be found by considering a sequence $\tau_i \downarrow 0$ and solving a sequence discrete-time problems of the form

$$\begin{aligned}\mu_i =& \min_{Q \in \mathcal{H}_2(D)} \|Q\|_{\mathcal{H}_2} \\ \text{subject to: } Q(z)|_{z=0} =& 0 \\ \left|(S_E^1(\tau_i) + S_E^2(\tau_i) * q)_k\right| \leq& \frac{M}{\tau_i} \\ k =& 0, 1 \ldots N-1 \\ \left|(S_E^1(\tau_i) + S_E^2(\tau_i) * q)_k\right| \leq& \frac{Me^{t_o/\tau_o}}{\tau_i}\left(1 - \frac{\tau}{\tau_o}\right)^{k-1} \\ k =& N, \ldots \\ N =& \left\lceil -\frac{t_o}{\tau\, Ln(1 - \frac{\tau}{\tau_o})} \right\rceil\end{aligned} \tag{4-10}$$

where $S_E^j(\tau_i)$ denotes the EAS corresponding to the transfer function S^j for the value τ_i, and where q is the impulse response of Q.

From the discussion above it follows that continuous time constrained $\mathcal{H}_2$ problems can be solved by solving a sequence of discrete time problems, using the techniques proposed in Section III. However, note that, when compared with Problem 1, (4-10) has an additional interpolation constraint, $Q(0) = 0$,

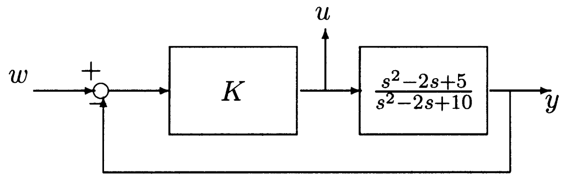

Fig. 4. Block diagram for a simple continuous-time example.

required to guarantee that the continuous time system has a finite $\mathcal{H}_2$ norm.

Next, we illustrate the effectiveness of this approach with a simple design problem. Consider the problem of minimizing the $\mathcal{H}_2$ norm of the complementary sensitivity function for the unstable nonminimum phase system shown in Fig. 4, subject to a constraint on the peak of the control action due to a unit-impulse disturbance w.

In this case, the optimal (unconstrained) $\mathcal{H}_2$ controller achieves $\|T_{yw}\|_{H_2} = 5.2$ with $\|T_{uw}\|_{\mathcal{L}^\infty} = 7.32$. Suppose that it is required that the magnitude of the control action in response to a unit-impulse disturbance must remain below 5, i.e., $\|T_{uw}\|_{\mathcal{L}^\infty} \leq 5$. Table I and Fig. 5(a) summarize the results obtained using the EAS approximation for different values of the parameter τ. Note that for $\tau \leq 0.01$ the gap is below 10% for the $\mathcal{H}_2$ norm and virtually zero for the $\mathcal{L}^\infty$ norm. Finally, Fig. 5(b) shows a comparison of the constrained versus the unconstrained impulse responses for the resulting (after model reduction) eigth-order controller. This controller meets the performance specifications while maintaining the settling time and $\|T_{yw}\|_2$ comparable to the unconstrained design.

V. APPLICATION: VISUAL TRACKING OF AN UNCOOPERATIVE TARGET

In this section, we illustrate the advantages of the proposed method by designing a controller for the active vision application described in Section I.

A. Background

In the past few years, active vision systems, i.e., systems incorporating feedback as an integral part of the loop, have emerged as a viable option for a large number of applications, ranging from MEMS manufacture [24] to vision assisted surgery [60], assisting individuals with disabilities [46], [58], and intelligent vehicle highway systems [45], [56]. In practice, using these systems in dynamic scenes requires both real-time visual processing and real-time closed-loop control. Recent hardware developments have make this now possible, leading to a number of systems [12], [14], [23], [38], [44].

Active vision systems appeared as far back as the late 1970s [30], with the main concern at that time being stability, which was often accomplished experimentally, by detuning the controller. An excellent survey of the earlier work and a comprehensive literature review up to 1996 can be found in [29]. Recent work has recognized the fact that robustness issues are central to the success of active vision systems. Robustness to calibration errors and estimation noise has been addressed in [26], [55], and [43] respectively. However, while in all these cases the control algorithm is relatively simple, it contains parameters that must be empirically tuned to achieve good performance. Robust tracking performance against calibration errors, variations in the optical parameters of the system and unmodeled dynamics has been addressed in [49], by using a combined model of the vision sensor and pan and tilt dynamics in an $\mathcal{H}_\infty/\mu$–synthesis framework. As standard in the μ–synthesis framework, here, performance is enforced through the use of appropriate weighting functions, whose tuning also entails a certain degree of trial-and-error experimentation.

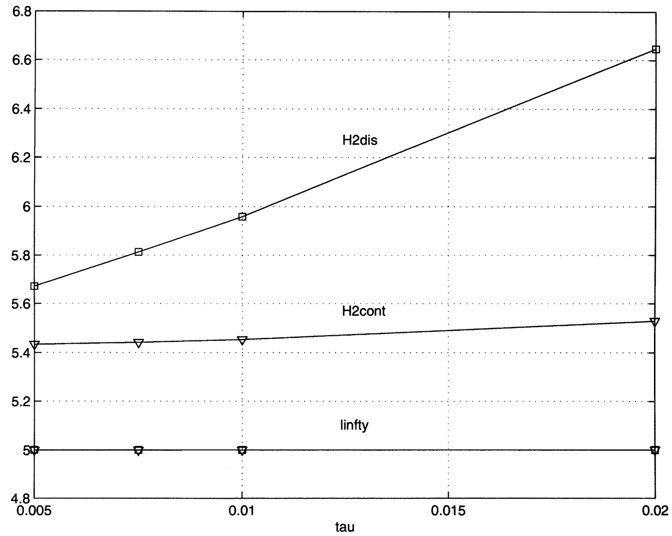

(a)

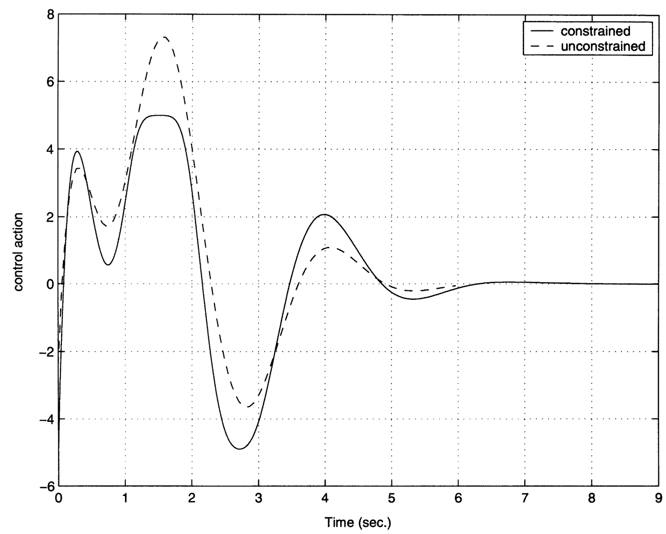

(b)

Fig. 5. Continuous-time example. (a) Approximation error for different values of τ. (b) Comparison of the control responses.

TABLE I
RESULT FOR THE CONTINUOUS–TIME EXAMPLE FOR DIFFERENT VALUES OF τ

τ	$\|\cdot\|_{2,EAS}$	$\|\cdot\|_{2,cont}$	$\|\cdot\|_{\ell^\infty,EAS}$	$\|\cdot\|_{\mathcal{L}^\infty,cont}$
0.02	6.647	5.529	4.999	5.0
0.01	5.959	5.454	4.999	5.0
0.0075	5.813	5.442	5.000	5.0
0.005	5.671	5.434	5.000	5.0

This section illustrates how time-domain performance specifications can be exactly addressed, without trial-and-error iterations, by using the $\mathcal{H}_2$ control with time domain constraints formalism. While at this point this represents only a first step toward this goal, since it guarantees only *nominal* performance, once these techniques prove to be useful, we plan to address robustness at a later date by combining them with the approach proposed in [54].

B. Hardware and Image Processing Description

The hardware setup used in this paper, shown in Fig. 6, consists of a BiSight robotic head equipped with two Hitachi KP-M1 cameras and Fujinon H10X11EMPX-31 lenses. The BiSight platform contains two dc brush drive motors, equipped with position encoders, that allow for rotational motion around the vertical (pan) and horizontal (tilt) axis, as illustrated in Fig. 6(a). These motors are driven using a 10-channel PMAC δ–τ controller. At its lowest level of operation, the PMAC contains, for each channel, a PID servo loop updated at 2.2 KHz, that drives the position of the corresponding motor to a desired setpoint (specified in motor encoder units). At a higher level, the PMAC contains a DSP processor that computes trajectories that interpolate desired points, and executes them by changing the setpoint of the corresponding channel. However, while this results in smooth motion, the delay incurred by the trajectory preplanning (up to 400 ms) is unnaceptable for real-time tracking (see [8] for details). In this research, we avoided this delay by driving the PMAC at the servo level, i.e., by directly accessing its position registers. Finally, the image processing required to capture the images and locate the target was performed using a Datacube MaxSPARC S250 hosted by a dual processor Sun Ultra 2 workstation, allowing for processing 512×512 pixel images at video rate (30 Hz). A block diagram of the complete system showing the interconnection of the various components is shown in Fig. 6(b).

Next, we briefly discuss the choice of the image processing algorithms used in this paper. The so called *"motion correspondence"* problem, i.e., to determine the image position of the object being tracked in the frames of the sequence-has been extensively studied in the computer vision literature, and a large number of techniques have been proposed, both for known and unknown objects (see, for instance, [2]–[4], [9], [14], [27], [29], [35], [38], [57], and the references therein). Correspondences between individual frames are usually integrated over time to exploit the dynamical properties of the target, using, for instance, Condensation trackers [3]. These trackers generalize Kalman-filter based ones by allowing more general (multi-modal) observation noise models, although in some cases can result on impractical computational requirements [32].

Selection of the image processing algorithm entails a compromise between complexity and robustness, since time delays stemming from more sophisticated image processing algorithms have negative impact on the stability and overall performance of the closed-loop system. Since the goal of the present paper is to concentrate on performance issues arising from hard time-domain constraints in the control action, we selected, as a compromise between complexity and robustness, a normalized cross-correlation with template update algorithm [35] to track the

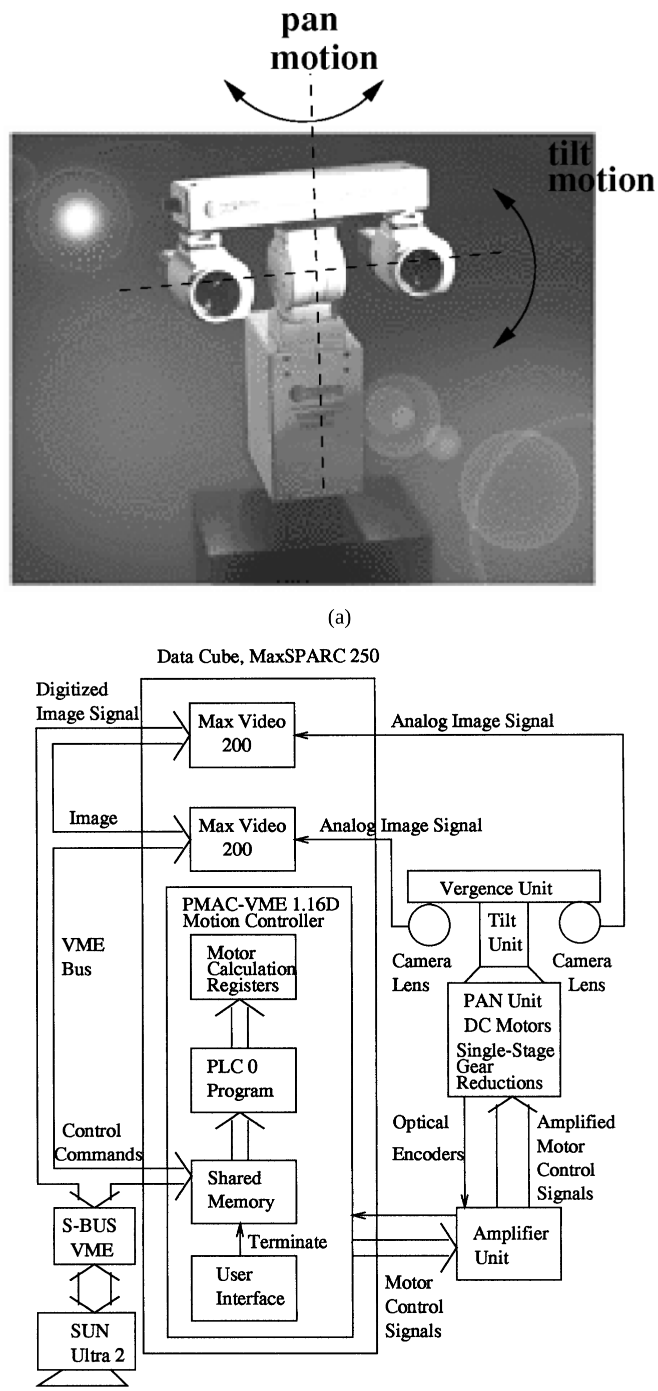

(a)

(b)

Fig. 6. (a) Experimental setup. (b) Corresponding block diagram.

target through a sequence of frames. As shown in the sequel (see also [31]), this algorithm achieves good performance tracking targets at video rate.

C. Control Objectives and Performance Specifications

Fig. 7 shows a block diagram of the augmented plant, where v_{target}, y_{target} and u represent the velocity and position (in the image plane) of the target, and the control input to the PMAC board, respectively. Here, the integrator preceding $\tilde{u}$, the input to the pan and tilt unit, models the way this board distributes setpoint changes across the sampling period to avoid jerky motion

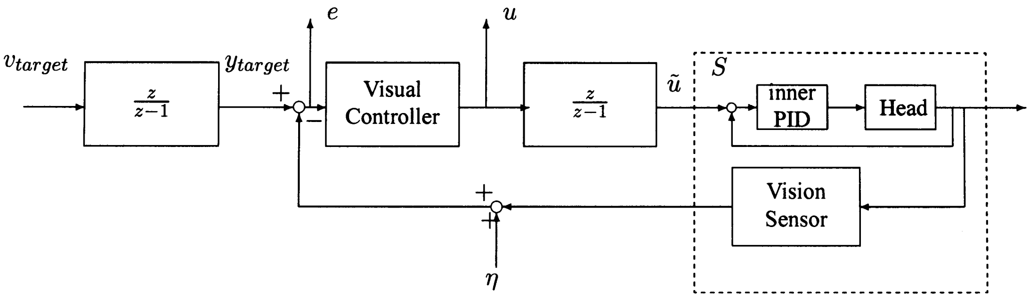

Fig. 7. Augmented plant for the active vision problem.

(see [31] for details). Finally, $e = (e_x, e_y)$ denotes the two-dimensional position in the image plane, relative to the center of the image, of the centroid of the target, corrupted by measurement noise $\eta = (\eta_x, \eta_y)$.

The goal is to minimize $||e||_2$, the RMS value of the displacement of the target from the center of the image, by rotating the head around its vertical (pan) and horizontal (tilt) axes. In addition, the closed loop system should satisfy the following specifications (motivated by physical considerations).

a) Zero steady-state tracking error to step inputs at y_{target} (i.e., impulse velocity inputs v_{target}). Note that this specification is automatically met by any internally stabilizing controller due to the integral action provided by the PMAC.
b) Small overshoot (less than 20%) and appropriate setting time (on the order of five sampling times) in both the error and control responses to a step input at y_{target}[1]
c) Closed-loop bandwidth of at least 4 radians/s (this roughly corresponds to targets moving at 4 m/s).
d) Control action to a step input at y_{target} of 25 pixels (roughly corresponding to a target moving with an angular velocity of 4 rad/s) not to exceed 50 control units (motor encoder counts), in order not to saturate the actuators.
e) Rejection of high frequency image processing noise η.

In the sequel, due to space limitations, we consider only the problem of designing a controller for the pan axis, since design of a controller for the tilt axis follows exactly along the same lines.

D. Plant Modeling

Applying the $\mathcal{H}_2$ control with time-domain constraints formalism to the active vision problem, requires reducing it to the form shown in Fig. 3. This entails finding a model P of the system that includes the dynamics of the head, the actuators, i.e., the low level PID servo loops that drive the motors, and the computer vision module[2] (the block labeled S in Fig. 7).

Control oriented identification of the plant, followed by a model (in)validation step, yielded the model for the nominal transfer function from $\tilde{u}$ to e_x, the horizontal displacement of the target, measured in pixels (see [49] for details), shown in the equation at the bottom of the page, where the factor $1/z^3$ models the delay due to the time required by the image processing algorithms to find the target in each frame.

E. Controller Design

In order to achieve the performance specifications given in Section V-C, our goal is to design a controller that achieves an RMS value of the tracking error, $||e||_2$, comparable to that achieved by the optimal $\mathcal{H}_2$ controller, while at the same time avoiding the large control action and oscillatory responses noted in the introduction. To this effect, we first carried-out a design where the control action in response to a step displacement of the target of 25 pixels was bounded by $||u||\ell^\infty \leq 50$ (roughly $1/3$ of the control action used by the optimal $\mathcal{H}_2$ controller). Note that, in this case, Theorem 3 is not directly applicable since S^{12} has a zero at $z = 1$ due to the integrator at the control input. However, as we show next the upper bound of the cost can still be computed using finite-dimensional optimization.

Consider the Youla parametrization obtained by selecting $K = \mathcal{F}_\ell(J, Q)$ with

$$J = \left(\begin{array}{c|c} A_j & B_j \\ \hline C_j & D_j \end{array}\right) \tag{5-1}$$

where (5-2)–(5-3), shown at the bottom of the next page, holds.

It can be easily verified that this choice renders T^{12} and T^{21} inner and co-inner respectively. Moreover, the controller corresponding to the following Q:

$$\begin{aligned} Q_{\text{FIR}} =& 0.7022 + 0.2593z^{-1} + 0.0194z^{-2} + 0.0076z^{-3} \\ &+ 0.0492z^{-4} + 0.0729z^{-5} \\ &+ 0.0522z^{-6} + 0.0172z^{-7} \end{aligned} \tag{5-4}$$

[1]These specifications are designed to prevent correlator walk off problems, i.e., the window used for the normalized cross correlation in the image processing drifting away from the true target.

[2]By identifying a single model combining the dynamics of the pan/tilt unit, actuators and the computer vision module, this approach avoids artificially inflating the order of the resulting model, and better captures their interaction.

$$P(z) = \frac{0.0359z^6 + 0.0419z^5 + 0.1289z^4 - 0.0468z^3 - 0.0366z^2 + 0.0002z + 0.0389}{1.0000z^6 - 0.3585z^5 + 0.3282z^4 - 0.1777z^3 + 0.1762z^2 - 0.0424z + 0.0345} \times \frac{1}{z^3}$$

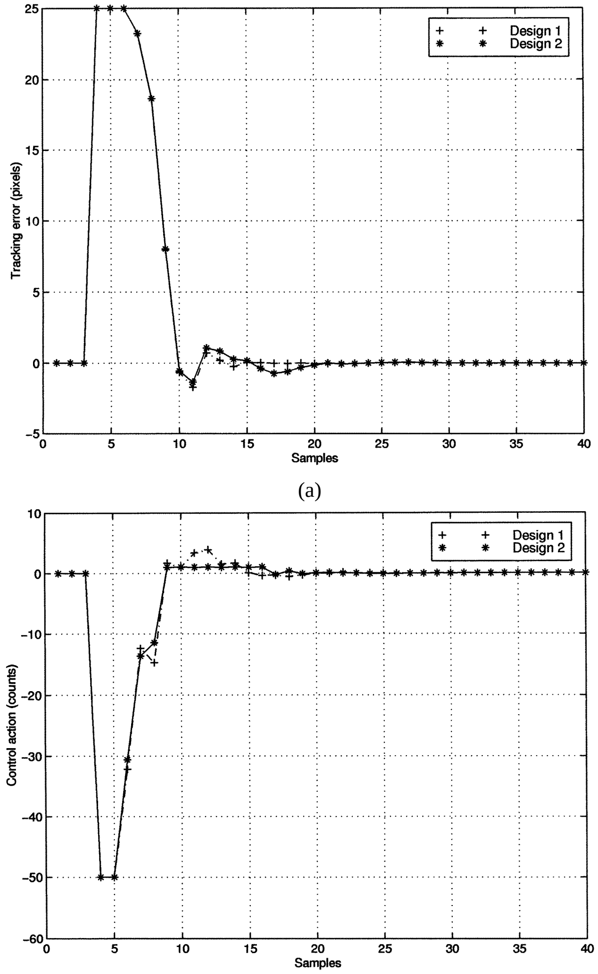

(a)

(b)

Fig. 8. Responses of the constrained controllers (simulation). (a) Tracking error. (b) Control action.

TABLE II
PERFOMANCE OF DIFFERENT $\mathcal{H}_2$ CONTROLLERS

method	contr. order	$\|T_{ey}\|_2$	Peak Control to Step in y
opt. $\mathcal{H}_2$	9	1.99	167.9
Design 1	10	2.13	50
Design 2	10	2.13	50

is feasible and yields $\|T_{ew}\|_2 = 2.13$. Since $\|Q\|_{\ell^\infty} \le \|Q\|_2$, it follows that the optimal solution to Problem 4 satisfies $|q_k| \le 2.13 \doteq M_Q$. Finally, direct computations show that for the choice of Youla parametrization given above we have that: $|S^1(k)| + \|(I - \mathcal{P}_k)S^2\|_{\ell^1} M_Q \le 2$ for all $k \ge 12$. Thus, it follows that $N = 12$ is a suitable horizon for the upper-bound computation. The corresponding controller was found by solving Problem 4 using the projection-based method implemented in Matlab's quadprog command for medium-sized problems [37].

Fig. 8 shows the control and error responses achieved by this controller in response to a step displacement of the centroid of the target of 25 pixels, relative to the center of the image. As shown there, the tracking error (the distance from the centroid of the target to the center of the image) settles very quickly, with little overshoot. Note however that the control action oscillates, settling down after 13 samples. To remove this oscillation, we carried out a second design, imposing the constraints: 1) $|u(k)| \le 50$ and 2) $|u(k)| \le 1$, $k \ge 9$. The resulting twenty-eigth-order controller was reduced to tenth order by using Hankel norm model reduction (the optimal $\mathcal{H}_2$ controller for this problem has order nine), leading to a controller with the state-space realization shown in (5-5) at the bottom of the next page.

$$A_j = \begin{pmatrix} 0.475 & -0.415 & 0.080 & -0.730 & -0.584 & -0.188 & -0.669 & -0.411 & -3.499 \\ 0.676 & -0.112 & 0.552 & 0.280 & 0.130 & -0.089 & -0.033 & -0.166 & -0.274 \\ -0.001 & 0.717 & 0.394 & -0.414 & -0.253 & -0.293 & -0.103 & -0.194 & -0.846 \\ -0.003 & 0.00 & 0.355 & -0.488 & -0.204 & -0.159 & -0.374 & -0.430 & -1.467 \\ -0.008 & 0.001 & 0.077 & 0.155 & -0.879 & -0.731 & -0.968 & -1.042 & -4.924 \\ -0.003 & 0.001 & 0.026 & -0.146 & 0.654 & -0.367 & -0.301 & -0.417 & -1.685 \\ -0.001 & 0.00 & 0.011 & -0.059 & -0.141 & 0.542 & 0.047 & -0.667 & -0.649 \\ 0 & 0 & 0 & 0 & 0 & 0 & 0 & 0.385 & -0.079 \end{pmatrix} \tag{5-2}$$

$$B_j = \begin{pmatrix} -0.056 & 5.110 \\ 0.015 & 0.442 \\ 0.031 & 1.248 \\ 0.020 & 2.226 \\ 0.056 & 7.305 \\ 0.096 & 2.474 \\ 0.288 & 1.000 \\ 0.275 & 0.000 \\ 1.346 & 0.000 \end{pmatrix}$$

$$D_j = \begin{pmatrix} 0 & 6.716 \\ 1.000 & 0 \end{pmatrix}$$

$$C_j = \begin{pmatrix} -0.008 & 0.001 & 0.071 & -0.395 & -0.944 & -0.538 & -0.934 & -0.838 & -4.538 \\ 0.000 & 0.000 & 0.000 & 0.000 & 0.000 & 0.000 & 0.000 & 0.000 & -0.743 \end{pmatrix}. \tag{5-3}$$

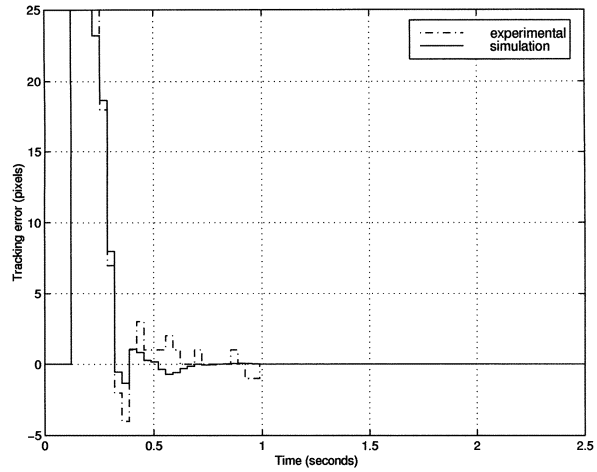

(a)

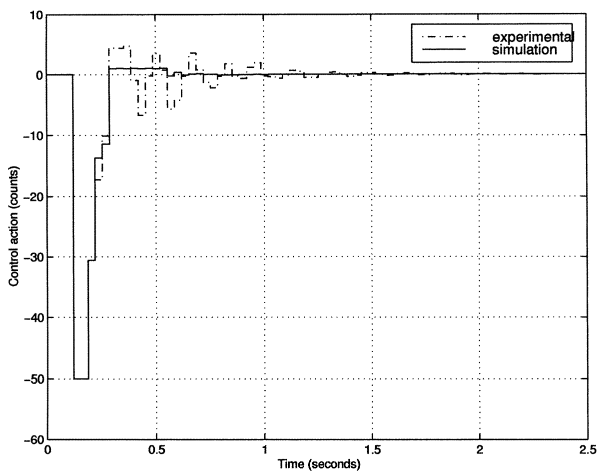

(b)

Fig. 9. Response of the constrained controller (design 2). (a) Tracking error. (b) Control action.

As shown in Figs. 8 (simulation) and 9 (experimental), this controller achieves an error response virtually identical to that of design 1, while removing the oscillations in the control action. The different designs are compared in Table II.

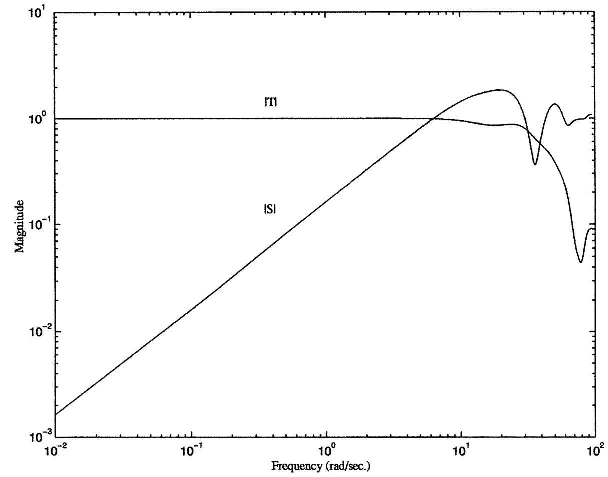

(a)

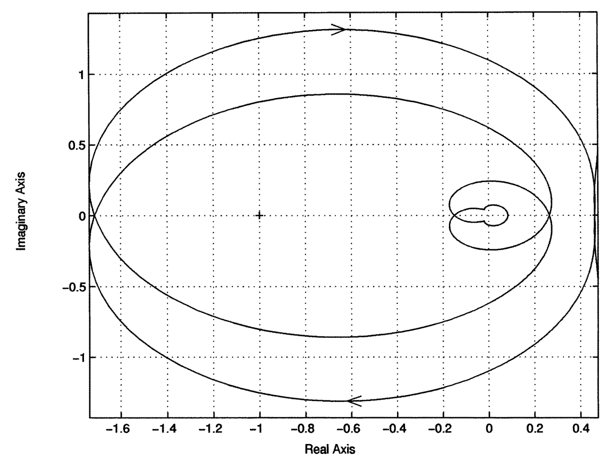

(b)

Fig. 10. Frequency responses achieved with the controller (5-5). (a) Sensitivity and complementary sensitivity. (b) Nyquist plot.

F. Controller Benchmarking

Fig. 10(a) shows the closed-loop sensitivity and complementary sensitivity achieved with the controller (5-5). Note that these transfer functions have bandwidths of 4 rad/s and 20 rad/s,

$$
\begin{aligned}
A_k &= \begin{pmatrix}
0.4245 & 0.8559 & -0.0524 & 0.0042 & -0.0504 & -0.0193 & 0.0092 & 0.0095 & -0.0048 & -0.0005 \\
-0.8559 & 0.2830 & -0.1090 & 0.0215 & -0.1168 & -0.0344 & 0.0172 & 0.0192 & -0.0091 & -0.0005 \\
0.0524 & -0.1090 & -0.5098 & -0.7446 & 0.2314 & -0.0658 & 0.0203 & 0.0040 & -0.0092 & -0.0051 \\
0.0042 & -0.0215 & 0.7446 & -0.5388 & -0.3139 & -0.0765 & 0.0346 & 0.0336 & -0.0177 & -0.0022 \\
-0.0504 & 0.1168 & -0.2314 & -0.3139 & -0.5185 & 0.3149 & -0.1169 & -0.0764 & 0.0562 & 0.0159 \\
0.0193 & -0.0344 & -0.0658 & 0.0765 & -0.3149 & -0.6183 & -0.2315 & -0.4180 & 0.0896 & -0.0458 \\
0.0092 & -0.0172 & -0.0203 & 0.0346 & -0.1169 & 0.2315 & 0.8361 & -0.3803 & 0.0206 & -0.0597 \\
-0.0095 & 0.0192 & 0.0040 & -0.0336 & 0.0764 & -0.4180 & 0.3803 & 0.2651 & 0.3831 & 0.2116 \\
-0.0048 & 0.0091 & 0.0092 & -0.0177 & 0.0562 & -0.0896 & 0.0206 & -0.3831 & -0.6531 & 0.4873 \\
0.0005 & -0.0005 & -0.0051 & 0.0022 & -0.0159 & -0.0458 & 0.0597 & 0.2116 & -0.4873 & -0.5989
\end{pmatrix} \\
B_k &= \begin{pmatrix} 0.5990 & 0.6535 & 0.3173 & 0.1155 & -0.4039 & 0.0825 & 0.0458 & -0.0580 & -0.0248 & -0.0002 \end{pmatrix}^T \\
C_k &= \begin{pmatrix} 0.5990 & -0.6535 & -0.3173 & 0.1155 & -0.4039 & -0.0825 & 0.0458 & 0.0580 & -0.0248 & 0.0002 \end{pmatrix} \\
D_k &= -2.0000.
\end{aligned}
\tag{5-5}
$$

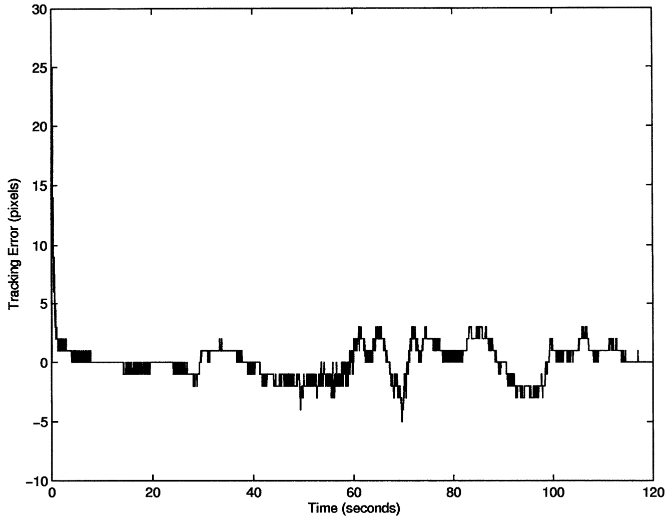

(a)

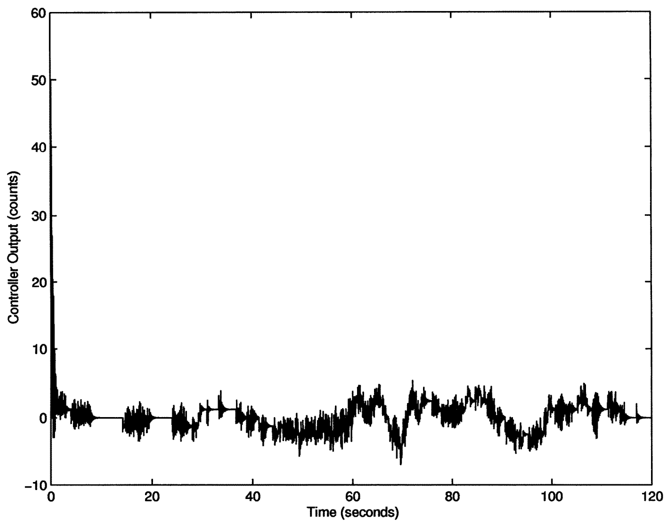

(b)

Fig. 11. Tracking error and control action in response to a random velocity profile (experimental).

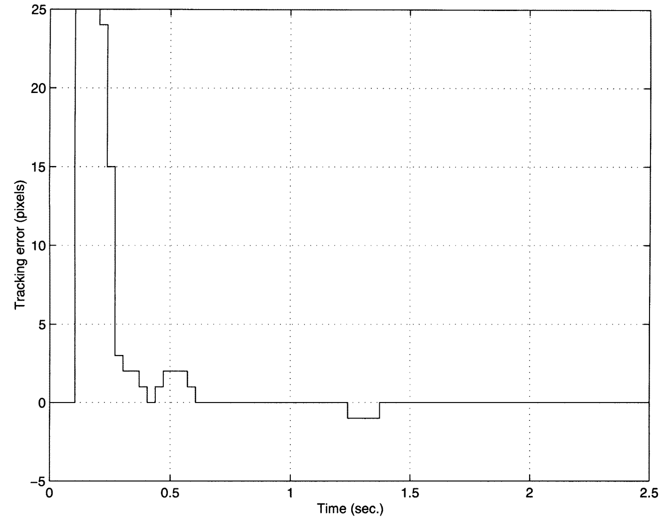

(a)

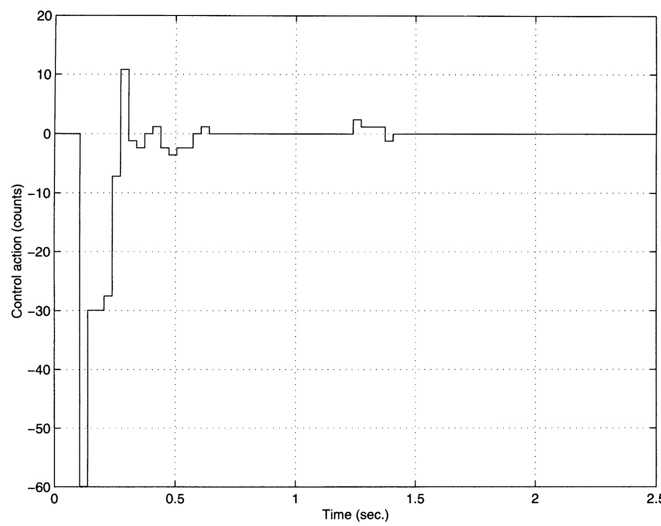

(b)

Fig. 12. Response of an empirically tuned PID controller. (a) Tracking error. (b) Control action (experimental).

respectively, and thus satisfy the performance specifications. Fig. 10(b) shows the Nyquist plot of the loop function, clearly displaying its nonminimum phase nature. The corresponding gain and phase margins are $GM = 4.7$ dB and $PM = 58.5^o$. Thus, in this case, even though the controller has not been designed taking robustness into account,[3] the closed-loop system has reasonably good robustness properties against gain variations, stemming from instance from changes in the optical parameters of the system, or phase variations, due for instances to variable time delays in the image processing.

Fig. 11 shows additional experimental results corresponding to a random target velocity profile v_{target}. As llustrated there, the closed-loop system is able to track the target, while using a moderate control action.

Finally, Fig. 12 shows the experimental step response obtained using a PID controller, empirically tuned to minimize the peak of the control action while maintaining a settling time comparable to that of the constrained $\mathcal{H}_2$ controller. It is worth mentioning that extensive trial and error iterations were needed to bring the control action down to 60 encoder units. Indeed, the best parameter combination was found by "reverse engineering" the constrained $\mathcal{H}_2$ controller. Moreover, no combination was found that further reduced the control action, subject to the settling time constraint.

[3]The proposed method inherits the potential fragility of optimal $\mathcal{H}_2$ control.

TABLE III
DESIGN 2 VERSUS PID

method	$\|T_{ey}\|_2$	$\|T_{u\eta}\|_2$	Peak Control to Step in y
Design 2	2.13	2.30	50
PID	2.12	2.86	60

Table III compares the performance of the constrained $\mathcal{H}_2$ and PID controllers. Both achieve virtually identical tracking error. However, the PID controller requires larger control actions both to track target motions and to reject noise.

VI. CONCLUSION

In this paper, we consider the problem of optimizing the $\mathcal{H}_2$ norm of a given system subject to additional specifications given in terms of the response to a given test signal. The main result shows that both in the discrete and continuous time cases this problem admits a solution in $\overline{\mathcal{RH}_2}$. Moreover, suboptimal solutions can be obtained by solving sequences of finite-dimensional quadratic programming problems until the gap between upper and lower bounds of the solution is smaller than a prespecified tolerance. Additional results show that the sequence of controllers thus obtained converges strongly to the optimal solution.

These results were illustrated with a practical example arising in the context of active vision and a simple academic example showing convergence of the sequence of approximations used to solve continuous time problems. Based on consistent numerical experience, it seems that for discrete-time SISO problems, whenever the constraint-level for the time-domain constraints is set above the minimally achievable ℓ^∞ norm, the optimal Q has a finite impulse response. However, at this point no formal proof of this conjecture is available.

APPENDIX
EULER APPROXIMATING SYSTEM AND ITS PROPERTIES

In the sequel, we summarize, for ease of reference, some properties of the EAS system relevant to the $\mathcal{H}_2$ with time-domain constraints problem.

Lemma 5: Consider the stable strictly proper system

$$G(s) = \left(\begin{array}{c|c} A & B \\ \hline C & 0 \end{array}\right) \tag{A-1}$$

and its corresponding EAS

$$G_E(z,\tau) = \left(\begin{array}{c|c} I+\tau A & \tau B \\ \hline C & 0 \end{array}\right) \tag{A-2}$$

where $\tau > 0$. Let $\tau_{\max} = \min_{\lambda\in\Lambda} 2{-}re(\lambda)/|\lambda|^2$ where Λ is the set of eigenvalues of A and consider a strictly decreasing sequence $\tau_{\max} > \tau_i \downarrow 0$. Then, the following properties hold.

1) $G_E(z,\tau_i)$ is asymptotically stable for all i.
2) $\|G\|^2_{\mathcal{H}_2} \leq (1/\tau_i)\|G_E(z,\tau_i)\|^2_{\mathcal{H}_2} \quad \forall i$.
3) $1/\tau_i\|G_E(z,\tau_i)\|^2_{\mathcal{H}_2} \geq (1/\tau_j)\|G_E(z,\tau_j)\|^2_{\mathcal{H}_2}, i<j$.
4) $\lim_{\tau_i\to 0}(1/\tau_i)\|G_E(z,\tau_i)\|^2_{\mathcal{H}_2} = \|G\|^2_{\mathcal{H}_2}$.
5) $\|g(t)\|_{\mathcal{L}^\infty} \leq (1/\tau)_i\|g_E(k,\tau_i)\|_{\ell^\infty} \quad \forall i$.
6) $\lim_{\tau_i\to 0}(1/\tau_i)\|g_E(k,\tau_i)\|_{\ell^\infty} = \|g(t)\|_{\mathcal{L}^\infty}$.

where $g(t)$ and $g_E(k,\tau)$ denote the impulse responses of (A-2) and its EAS, respectively.

Proof: The proof of items 1), 5), and 6) can be found in [48]. The proof of items 2)–4) is given in [1].

ACKNOWLEDGMENT

The authors are indebted to the anonymous reviewers for many suggestions to improve the original manuscript.

REFERENCES

[1] T. Amishima, "Multiobjective robust control: $\mathcal{H}_2$ related problems," Ph.D. dissertation, The Pennsylvania State University, University Park, PA, 1999.
[2] M. J. Black and A. D. Jepson, "Eigentracking: Robust matching and tracking of articulated objects using a view-based representation," *Int. J. Comp. Vision*, vol. 26, no. 1, pp. 63–84, 1998.
[3] B. North, A. Blake, M. Isard, and J. Rittscher, "Learning and classification of complex dynamics," *IEEE Trans. Pattern Anal. Machine Intell.*, vol. 22, pp. 1016–1034, Sept. 2000.
[4] A. Blake and M. Isard, *Active Contours*. Berlin, Germany: Springer-Verlag, 1998.
[5] F. Blanchini, S. Miani, and M. Sznaier, "Robust performance with fixed and worst case signals for uncertain time-varying systems," *Automatica*, vol. 33, no. 12, pp. 2183–2189, 1997.
[6] F. Blanchini and M. Sznaier, "Rational $\mathcal{L}^1$ suboptimal compensators for continuous–time systems," *IEEE Trans. Automat. Contr.*, vol. 39, pp. 1487–1492, July 1994.
[7] F. Blanchini, "Set invariance in control," *Automatica*, vol. 35, no. 11, pp. 1747–1767, Nov. 1999.
[8] U. M. Cahn Von Seelen, "Performance evaluation of an active vision system," Ph.D. dissertation, Univ. Pennsylvania, Philadelphia, PA, 1997.
[9] E. Calabi, P. J. Olver, C. Shakiban, A. Tannenbaum, and S. Haker, "Differential and numerically invariant signature curves applied to object recognition," *Int. J. Comp. Vision*, vol. 26, no. 2, pp. 107–135, 1998.
[10] E. Castelan and S. Tarbouriech, "On positive invariance and output feedback stabilization of input constrained linear systems," *Proc. 1994 Amer. Control Conf.*, pp. 2740–2744, 1994.
[11] D. Chmielewski and V. Manousiouthakis, "On constrained infinite-time linear quadratic optimal control," *Syst. Control Lett.*, vol. 29, no. 3, pp. 121–129, 1996.
[12] J. J. Clark and N. J. Ferrier, "Modal control of an attentive vision system," in *Proc. 1988 Int. Conf. Computer Vision*, pp. 514–523.
[13] M. Cotlar and R. Cignoli, *An Introduction to Functional Analysis*. Amsterdam, The Netherlands: North-Holland, 1974.
[14] D. Coombs and C. Brown, "Real-time binocular smooth pursuit," *Int. J. Comp. Vision*, vol. 11, no. 2, pp. 147–164, 1993.
[15] M. A. Dahleh and J. B. Pearson, "l^1—Optimal feedback controllers for MIMO discrete–time systems," *IEEE Trans. Automat. Contr.*, vol. AC-32, pp. 314–322, Apr. 1987.
[16] ——, "$\mathcal{L}^1$—Optimal compensators for continuous–time systems," *IEEE Trans. Automat. Contr.*, vol. AC-32, pp. 889–895, Oct. 1987.
[17] ——, "Optimal rejection of persistent disturbances, robust stability, and mixed sensitivity minimization," *IEEE Trans. Automat. Contr.*, vol. 33, pp. 722–731, Aug. 1988.
[18] ——, "Minimization of a regulated response to a fixed input," *IEEE Trans. Automat. Contr.*, vol. 33, pp. 924–930, Oct. 1988.
[19] I. J. Diaz–Bobillo and M. A. Dahleh, "Minimization of the maximum peak-to-peak gain: The general multiblock problem," *IEEE Trans. Automat. Contr.*, vol. 38, pp. 1459–1482, Oct. 1993.
[20] C. E. T. Dorea and B. E. Milani, "Design of LQ regulators for state constrained continuous–time systems," *IEEE Trans. Automat. Contr.*, vol. 40, pp. 544–548, Mar. 1995.
[21] J. Doyle, K. Glover, P. Khargonekar, and B. Francis, "State-space solutions to standard $\mathcal{H}_2$ and $\mathcal{H}_\infty$ control problems," *IEEE Trans. Automat. Contr.*, vol. 34, pp. 831–846, Aug. 1989.
[22] N. Elia, P. M. Young, and M. A. Dahleh, "Robust performance for fixed inputs," in *Proc. 33rd IEEE Conf. Decision Control*, Lake Buena Vista, FL, Dec. 1994, pp. 2690–2695.
[23] B. Espiau, F. Chaumette, and P. Rives, "A new approach to visual servoing in robotics," *IEEE Trans. Robot. Automat.*, vol. 8, pp. 313–326, Mar. 1992.
[24] J. Feddema, "Microassembly of micro-electromechanical systems (MEMS) using visual servoing," presented at the Block Island Workshop Vision Control, Block Island, RI, 1997.
[25] P. O. Gutman and P. Hagander, "A new design of constrained controllers for linear systems," *IEEE Trans. Automat. Contr.*, vol. AC-30, pp. 22–33, Jan. 1985.
[26] G. Hager, "A modular system for robust positioning using feedback from stereo vision," *IEEE Trans. Robot. Automat.*, vol. 13, pp. 582–595, Apr. 1997.
[27] G. Hager and P. Belhumeur, "Efficient region tracking with parametric models of geometry and illumination," *IEEE Trans. Pattern Anal. Machine Intell.*, vol. 20, pp. 1025–1039, Oct. 1997.
[28] K. Hashimoto and H. Kimura, "LQ optimal and nonlinear approaches to visual servoing," in *Visual Servoing*, K. Hashimoto, Ed. Singapore: World Scientific, 1993, vol. 7, World Scientific Series in Robotics and Automated Systems, pp. 165–198.

[29] S. Hutchinson, G. D. Hager, and P. I. Corke, "A tutorial on visual servo control," *IEEE Trans. Robot. Automat.*, vol. 12, pp. 651–670, May 1996.
[30] J. Hill and W. T. Park, "Real time control of a robot with a mobile camera," in *Proc. 9th ISIR*, Washington, DC, Mar. 1979, pp. 233–246.
[31] T. Inanc, M. Sznaier, and O. Camps, "Synthesizing robust active vision systems: A combined robust identification/ μ-synthesis approach," presented at the 2002 IFAC World Congr., Barcelona, Spain, 2002.
[32] P. Jensfelt, O. Wijk, D. J. Austin, and M. Andersson, "Experiments on augmenting condensation for mobile robot localization," in *Proc. 2000 Int. Conf. Robotics Automation*, San Francisco, CA, Apr. 2000, pp. 2518–2524.
[33] T. Kailath, *Linear Systems*. Upper Saddle River, NJ: Prentice-Hall, 1980.
[34] M. Khammash, "Robust performance: Unknown disturbances and fixed inputs," *IEEE Trans. Automat. Contr.*, vol. AC-42, pp. 1730–1734, Dec. 1987.
[35] R. Jain, R. Kasturi, and B. G. Schunck, *Machine Vision*. New York: McGraw-Hill, 1995.
[36] D. Q. Mayne and H. Michalska, "Receding horizon control of nonlinear systems," *IEEE Trans. Automat. Contr.*, vol. 35, pp. 814–824, July 1990.
[37] *Optimization Toolbox*, The MathWorks, Inc., Natick, MA, 2001.
[38] I. D. Reid and W. Murray, "Active tracking of foveated feature clusters using affine structure," *Int. J. Comp. Vision*, vol. 18, no. 1, pp. 41–60, 1996.
[39] N. P. Papanikolopoulos, P. K. Khosla, and T. Kanade, "Visual tracking of a moving target by a camera mounted on a robot: A combination of control and vision," *IEEE Trans. Robot. Automat.*, vol. 9, pp. 14–35, Jan. 1993.
[40] M. Rotea, "The generalized $\mathcal{H}_2$ control problem," *Automatica*, vol. 29, no. 2, pp. 373–385, 1993.
[41] M. V. Salapaka and M. Dahleh, *Multiple Objective Control Synthesis*. London, U.K.: Springer-Verlag, 2000, vol. 252, Lecture Notes in Control and Information Sciences.
[42] P. Scokaert and J. Rawlings, "Constrained linear quadratic regulation," *IEEE Trans. Automat. Contr.*, vol. 43, pp. 1163–1169, Aug. 1998.
[43] O. Shakernia, Y. Ma, T. J. Koo, J. Hespanha, and S. S. Sastry, "Vision guided landing of an unmanned air vehicle," *Proc. 1999 IEEE Conf. Decision Control*, pp. 4143–4148, Dec. 1999.
[44] P. M. Sharkey, D. W. Murray, S. Vandevelde, I. D. Reid, and P. F. McLauchlan, "A modular head/eye platform for real-time reactive vision," *Mechatronics*, vol. 3, no. 4, pp. 517–535, 1993.
[45] C. E. Smith, C. A. Richards, S. A. Brandt, and N. P. Papanikolopoulos, "Visual tracking for intelligent vehicle-highway systems," *IEEE Trans. Veh. Technol.*, vol. 45, pp. 744–759, Apr. 1996.
[46] T. Starner and A. Pentland, "Real-time american sign language recognition using desk and wearable computer based video," *IEEE Trans. Pattern Anal. Machine Intell.*, vol. 20, pp. 1371–1375, Dec. 1998.
[47] M. Sznaier and T. Amishima, "$\mathcal{H}_2$ control with time domain constraints," in *Proc. 1998 Amer. Control Conf.*, 1998, pp. 3229–3233.
[48] M. Sznaier and F. Blanchini, "Mixed $\mathcal{L}^\infty/\mathcal{H}_\infty$ suboptimal controllers for continuous-time systems," *IEEE Trans. Automat. Contr.*, vol. 40, pp. 1831–1840, Nov. 1995.
[49] M. Sznaier, T. Inanc, and O. Camps, "Robust controller design for active vision systems," in *Proc. 2000 Amer. Control Conf.*, July 2000, pp. 2013–2017.
[50] M. Sznaier and M. J. Damborg, "Suboptimal control of linear systems with state and control inequality constraints," in *Proc of 26th IEEE Conf. Decision Control*, Los Angeles, CA, Dec. 1987, pp. 761–762.
[51] M. Sznaier and M. Damborg, "Heuristically enhanced feedback control of constrained discrete time linear systems," *Automatica*, vol. 26, no. 3, pp. 521–532, May 1990.
[52] M. Sznaier, "A set induced norm approach to the robust control of constrained linear systems," *SIAM J. Control Optim.*, vol. 31, no. 3, pp. 733–746, 1993.
[53] R. S. S. Pena and M. Sznaier, *Robust Systems Theory and Applications*. New York: Wiley, 1998.
[54] M. Sznaier, T. Amishima, P. Parrilo, and J. Tierno, "A convex approach to robust $\mathcal{H}_2$ performance analysis," *Automatica*, vol. 38, pp. 957–966, June 2002.
[55] C. Taylor, J. Ostrowski, and S. H. Jung, "Robust visual servoing based on relative orientation," presented at the Conf. Computer Vision Pattern Recognition, Fort Collins, CO, July 1999.
[56] C. J. Taylor, J. Kosecka, R. Blasi, and J. Malik, "Comparative study of vision-based lateral control strategies for autonomous highway driving," *Int. J. Robot. Res.*, vol. 18, no. 5, pp. 442–453, 1999.
[57] T. Thorhallsson and D. W. Murray, "Tensors of three affine views," in *Proc. Conf. Computer Vision Pattern Recognition*, Fort Collins, CO, pp. 450–456.
[58] J. K. Tsotsos, G. Verghese, S. Dickinson, M. Jenkin, A. Jepson, E. Milios, F. Nuflo, S. Stevenson, M. Black, D. Metaxas, S. Culhane, Y. Ye, and R. Mannn, "PLAYBOT: A visually-guided robot for physically disabled children," *Image Vision Comput.*, vol. 16, no. 4, pp. 275–292, Apr. 1998.
[59] M. Vassilaki, J. C. Hennet, and G. Bitsoris, "Feedback control of discrete-time systems under state and control constraints," *Int. J. Control*, vol. 47, no. 6, pp. 1727–1735, 1988.
[60] Y. F. Wang, D. R. Uecker, and Y. Wang, "Choreographed scope maneuvering in robotically-assisted laparoscopy with active vision guidance," in 3rd IEEE Workshop Applications Computer Vision, Sarasota, FL, Dec. 1996.
[61] Z. Q. Wang and M. Sznaier, "Rational $\mathcal{L}^\infty$-suboptimal controllers for SISO continuous time systems," *IEEE Trans. Automat. Contr.*, vol. 41, pp. 1358–1363, Sept. 1996.
[62] G. F. Wredenhagen and P. R. Belanger, "Piecewise-linear LQ control for systems with input constraints," *Automatica*, vol. 30, no. 3, pp. 403–416, 1994.
[63] K. Zhou, J. Doyle, and K. Glover, *Robust and Optimal Control*. Upper Saddle River, NJ: Prentice-Hall, 1995.

Mario Sznaier received the Ingeniero Electronico and Ingeniero en Sistemas de Computacion degrees from the Universidad de la Republica, Uruguay, and the MSEE and Ph.D. degrees from the University of Washington, Seattle, in 1983, 1984, 1986, and 1989, respectively.

From 1991 to 1993, he was an Assistant Professor of Electrical Engineering at the University of Central Florida, Orlando. In 1993, he joined the Pennsylvania State University, University Park, where he is currently a Professor of Electrical Engineering. He has also held visiting appointments at the California Institute of Technology, Pasadena, in 1990 and 2000. His research interest include multiobjective robust control; and H-infinity, control theory, control oriented identification, and active vision.

Takeshi Amishima received the M.Sc. degree from West Virginia University, Morgantown, and the Ph.D. degree from Pennsylvania State University, University Park, both in electrical engineering, in 1995 and 1999, respectively.

Since 1999, he has been with Mitsubishi Electric Corporation, Japan, working in the area of target tracking for air surveillance radars. His research interests include robust control, estimation theory, and target tracking.

Tamer Inanc was born in Izmir, Turkey, in 1970. He received the B.S. degree in electrical and electronics engineering from Dokuz Eylul University, Izmir, Turkey, and the M.S. and Ph.D. degrees in electrical engineering from the Pennsylvania State University, University Park, in 1991, 1996, and 2002, respectively.

He is currently a Postdoctoral Scholar at The California Institute of Technology, Pasadena, working on nonlinear trajectory generation for the cooperative path planning of multivehicle systems. His research interests are coordination of multivehicle systems, robust identification, robust control, robust active vision systems, and computer vision.